REGULAR PAPER

The sodium channel Na$_V$1.5 impacts on early murine embryonic cardiac development, structure and function in a non-electrogenic manner

Gerard A. Marchal[1] 🆔 | Arie O. Verkerk[1,2] | Rajiv A. Mohan[1,2] | Rianne Wolswinkel[1] |
Bastiaan J. D. Boukens[2] | Carol Ann Remme[1] 🆔

[1]Department of Experimental Cardiology, Amsterdam UMC (location Academic Medical Center), Amsterdam, the Netherlands

[2]Department of Medical Biology, Amsterdam UMC (location Academic Medical Center), Amsterdam, the Netherlands

Correspondence
Carol Ann Remme, Department of Experimental Cardiology, Amsterdam UMC (location Academic Medical Center), Room K2-104.2, Meibergdreef 15, 1105AZ Amsterdam, the Netherlands.
Email: c.a.remme@amsterdamumc.nl

Abstract

Aim: The voltage-gated sodium channel Na$_V$1.5, encoded by *SCN5A,* is essential for cardiac excitability and ensures proper electrical conduction. Early embryonic death has been observed in several murine models carrying homozygous *Scn5a* mutations. We investigated when sodium current (I_{Na}) becomes functionally relevant in the murine embryonic heart and how *Scn5a*/Na$_V$1.5 dysfunction impacts on cardiac development.

Methods: Involvement of Na$_V$1.5-generated I_{Na} in murine cardiac electrical function was assessed by optical mapping in wild type (WT) embryos (embryonic day (E)9.5 and E10.5) in the absence and presence of the sodium channel blocker tetrodotoxin (30 μmol/L). I_{Na} was assessed by patch-clamp analysis in cardiomyocytes isolated from WT embryos (E9.5-17.5). In addition, cardiac morphology and electrical function was assessed in *Scn5a*-1798insD$^{-/-}$ embryos (E9.5-10.5) and their WT littermates.

Results: In WT embryos, tetrodotoxin did not affect cardiac activation at E9.5, but slowed activation at E10.5. Accordingly, patch-clamp measurements revealed that I_{Na} was virtually absent at E9.5 but robustly present at E10.5. *Scn5a*-1798insD$^{-/-}$ embryos died in utero around E10.5, displaying severely affected cardiac activation and morphology. Strikingly, altered ventricular activation was observed in *Scn5a*-1798insD$^{-/-}$ E9.5 embryos before the onset of I_{Na}, in addition to reduced cardiac tissue volume compared to WT littermates.

Conclusion: We here demonstrate that Na$_V$1.5 is involved in cardiac electrical function from E10.5 onwards. *Scn5a*-1798insD$^{-/-}$ embryos displayed cardiac structural abnormalities at E9.5, indicating that Na$_V$1.5 dysfunction impacts on embryonic cardiac development in a non-electrogenic manner. These findings are potentially relevant for understanding structural defects observed in relation to Na$_V$1.5 dysfunction.

KEYWORDS

cardiac morphology, development, embryonic lethality, non-electrogenic, *SCN5A*, sodium current

---

ACTA PHYSIOLOGICA

1 | INTRODUCTION

Voltage-gated sodium channels are essential for cardiac excitability and propagation of electrical activity through the heart. Sodium channels consist of a transmembrane α-subunit and a modulatory β-subunit. The $Na_V1.5$ isoform of the α-subunit, encoded by *SCN5A*, is most abundant in cardiac tissue. Mutations in *SCN5A* are linked to various clinical syndromes associated with a high risk for arrhythmias and sudden cardiac death, including Long QT syndrome type 3 (LQTS3), Brugada syndrome and cardiac conduction disease.[1] These electrical phenotypes are explained by alterations in sodium current (I_{Na}) density and/or biophysical properties consequent to the mutation. However, structural abnormalities have also been observed in hearts from patients carrying *SCN5A* mutations and mice with heterozygous *Scn5a* deficiency.[2-8] Previous findings by Chopra and colleagues (2010) indicated that reduced *Scn5a* expression in zebrafish impacts on cardiac structural development independent of I_{Na}, indicating a potential non-electrogenic role for $Na_V1.5$.[9] Elucidation of the (non-)electrogenic mechanisms underlying this modulatory effect of $Na_V1.5$ on cardiac structure is essential given its potential significance for arrhythmogenesis.

Mice with homozygous deletion of *Scn5a* or carrying a homozygous *Scn5a* mutation have been shown to be embryonically lethal, dying around embryonic day (E)10.5.[10,11] While cardiac structural abnormalities were observed in homozygous *Scn5a*$^{-/-}$ mouse embryos, it remains unclear whether embryonic death of *Scn5a*$^{-/-}$ mice is because of electrogenic effects or non-electrogenic effects of *Scn5a*/$Na_V1.5$ on embryonic cardiac development, or a combination of both. For this, the exact point in embryonic development where I_{Na} becomes functionally relevant for cardiac electrical function and conduction needs to be elucidated. Sodium channels have been shown to be expressed in embryonic murine heart as early as E8.5-9.5.[12-14] However, the relatively depolarized membrane potential of cardiomyocytes during early embryonic stages likely renders sodium channels (partly) inactive.[15,16] Indeed, the sodium channel blocker tetrodotoxin (TTX) did not affect heart rate at E8.5-9.0.[13] Using patch clamp methodology, Davies (1996) and Mohan (2018) showed presence of I_{Na} in embryonic cardiomyocytes at E11.0 and E10.5 respectively, but similar experiments at earlier stages were not performed.[17,18]

We here investigated at which embryonic stage I_{Na} becomes functionally relevant for cardiac electrical function, and explored the potential non-electrogenic effects of sodium channel dysfunction on early cardiac development by studying morphology and function in embryos homozygous for the *Scn5a*-1798insD mutation. Combining electrophysiological measurements with histological assessments, we demonstrate that homozygous *Scn5a*-1798insD$^{-/-}$ embryos die at an early developmental stage and display cardiac abnormalities before

$Na_V1.5$ is involved in normal cardiac electrical activity and hence provide evidence for a non-electrogenic role for $Na_V1.5$ in cardiac development.

# 2 | RESULTS

2.1 | I_{Na} is functionally relevant for cardiac conduction from E10.5 onwards

We first explored cardiac conduction properties and the functional relevance of I_{Na} during early cardiac development (E9.5-10.5) in wild type (WT) hearts and isolated cardiomyocytes. Optical mapping recordings on isolated hearts revealed a significant decrease in ventricular activation time between E9.5 (14.2 ± 0.7 ms, n = 3) and E10.5 (4.9 ± 0.5 ms, n = 14; $P < .0001$), demonstrating faster conduction at E10.5 (Figure 1A,B). In line with this, the slope of the upstroke of the action potential (dV dt^{-1}) increased between E9.5 (2.7 ± 1.0 mV s^{-1}, n = 3) and E10.5 (6.8 ± 0.5 mV s^{-1}, n = 14; $P < .01$, Figure 1C) and the duration between onset and peak of the action potential became shorter between E9.5 (13.6 ± 0.9 ms, n = 3) and E10.5 (9.5 ± 0.1 ms, n = 14; $P < .01$). Overall, these results indicate increased sodium channel availability at E10.5 as compared to E9.5.

To assess the functional relevance of I_{Na} for cardiac activation at E9.5 and E10.5, the sodium channel blocker tetrodotoxin (TTX, 30 μmol/L) was used on WT hearts. Optical mapping recordings at E10.5 showed a significant increase in ventricular activation time after TTX (baseline [BL]: 7.2 ± 0.6 ms vs TTX: 19.3 ± 1.6 ms, n = 3; $P < .05$, Figure 1D,E). Accordingly, maximum dV dt^{-1} significantly decreased after TTX (BL: 9.0 ± 0.6 mV s^{-1} vs TTX: 3.5 ± 0.6 mV s^{-1}, n = 3; $P < .05$, Figure 1F). Because of the small size of the heart, measurements following TTX administration were not feasible at E9.5. However, video recordings of E9.5 intact embryos revealed that 30 μmol/L TTX affected neither heart rate (BL: 52.7 ± 11.0 beats per minute [BPM] vs TTX: 46.0 ± 7.9 BPM, n = 7; $P = NS$) nor ventricular beat duration, a measure of ventricular activation (BL: 677.3 ± 58.1 ms vs TTX: 731.9 ± 98.3 ms, n = 8; $P = NS$, Figure 1G,H), indicating that I_{Na} does not contribute to cardiac electrical function at this developmental stage. In contrast, administration of the L-type calcium channel inhibitor nifedipine (5 μmol/L) completely eradicated cardiac activity, demonstrating that cardiac electrical activity depends on calcium at E9.5 (Figure 1G).

Patch-clamp experiments showed that cardiomyocytes at E9.5 are able to generate a very small rapidly activating and inactivating I_{Na} upon clamping the membrane potential to −40 mV after a −100 mV hyperpolarizing step (−5.1 ± 1.3 pA pF^{-1}, n = 6, Figure 2A-C). However, this current is likely not physiologically relevant at E9.5 since
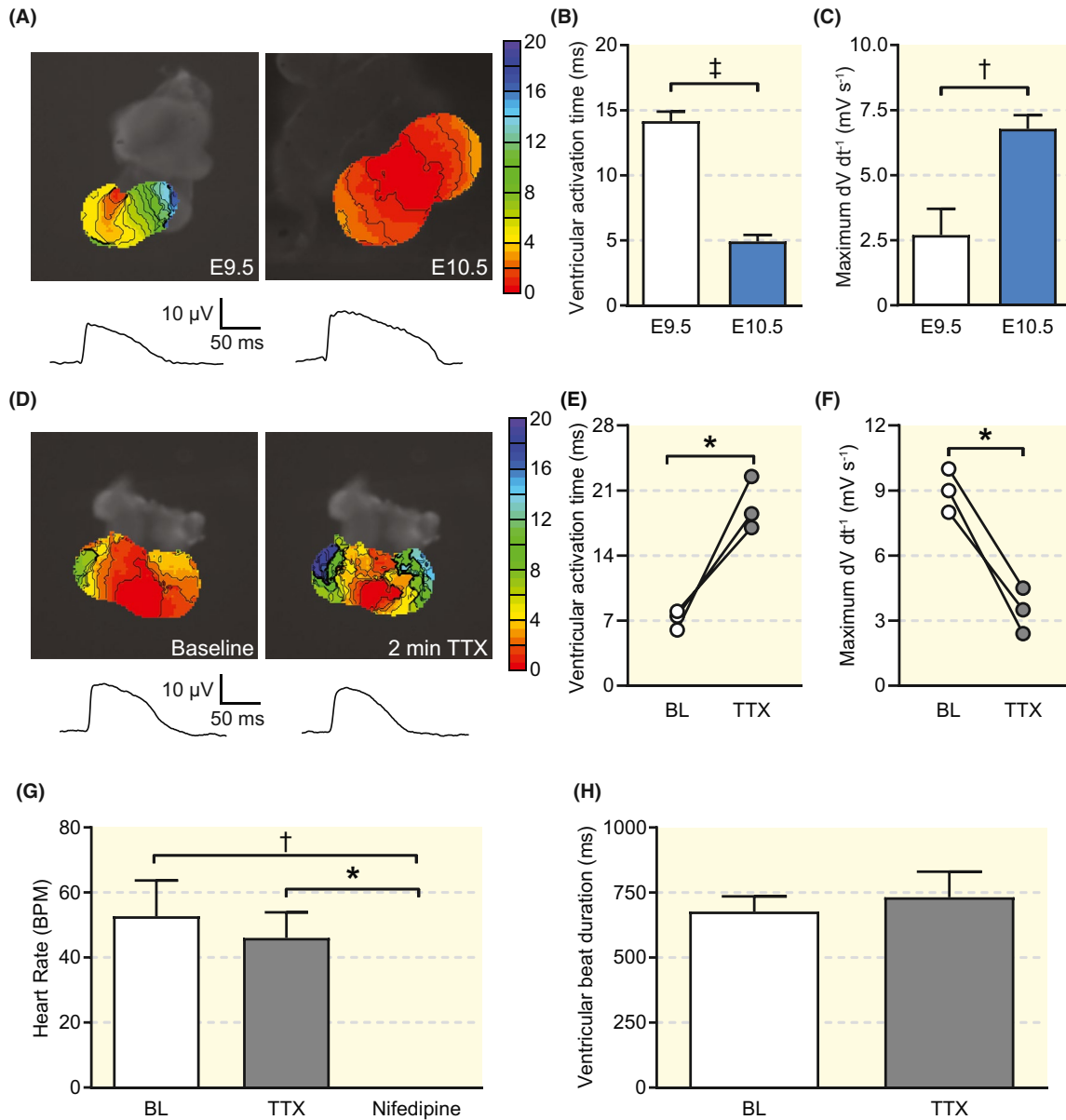
FIGURE 1 Progression of ventricular activation and I_{Na} during (early) embryonic development. A-C, Advancement of ventricular activation between E9.5 (n = 3) and E10.5 (n = 14). Typical examples of optical activation maps and action potentials measured E9.5 and E10.5 hearts (A). Average ventricular activation time (B) and maximum action potential upstroke velocity (maximum dV dt^{-1} in ventricles (C) at E9.5 and E10.5. D-F, Effect of 30 μmol/L tetrodotoxin (TTX) on ventricular activation at E10.5. Typical examples of optical maps and action potentials at baseline and after 2 min of TTX incubation (D). Average ventricular activation time (E) and maximum action potential upstroke velocity (maximum dV dt^{-1}), (F) at baseline and after TTX (n = 3). G and H, Effect of pharmacological ion channel blockade on cardiac activity in whole E9.5 embryos (n = 7). Effect of 2-minute TTX (30 μmol/L) and nifedipine (5 μmol/L) incubation on heart rate (G), and ventricular beat duration (H). *$P < .05$, †$P < .01$, ‡$P < .0001$ (unpaired t test (B and C), paired t test (E and F), Friedman test with Dunn's multiple comparisons test (G))

sodium channels are in a closed state (Figure 2C) at the measured maximum diastolic potential (MDP, -37.3 ± 4.4 mV, n = 7). In contrast, patch-clamp experiments at E10.5 revealed a substantially larger I_{Na} density (-36.4 ± 7.0 pA pF^{-1}, n = 7; $P < .01$) in addition to a more hyperpolarized MDP (-63.1 ± 2.2 mV, n = 7; $P < .0001$), as compared to E9.5 (Figure 2A-D). Measurements up to E17.5 show that throughout development an increasingly larger I_{Na} is generated in cardiomyocytes, while the MDP further hyperpolarizes

(Figure 2C,D). Thus, I_{Na} is functionally relevant for cardiac activation from E10.5 onwards.

2.2 | Homozygous *Scn5a*-1798insD embryos die during early embryonic development

We next investigated embryonic survival, cardiac electrical function and development in homozygous
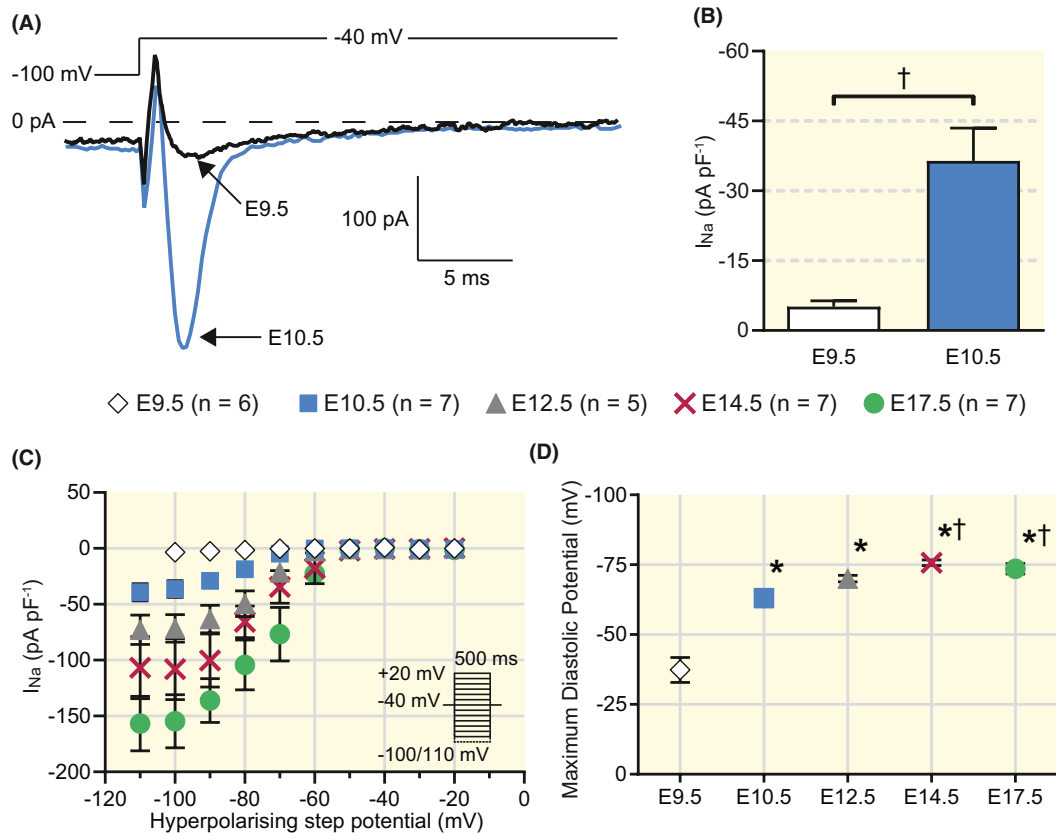
FIGURE 2 Patch-clamp analysis on isolated cardiomyocytes through development. A, Typical examples of peak I_{Na} density measurements in E9.5 and E10.5 cardiomyocytes. B, Average I_{Na} measured at −40 mV after clamping the membrane potential to −100 mV in cardiomyocytes from E9.5 (n = 6) and E10.5 (n = 7) embryos. C, Current-voltage plot of I_{Na} at −40 mV after a variable hyperpolarising step in cardiomyocytes at E9.5-E17.5. D, Average Maximum Diastolic Potential (MDP) measured in cardiomyocytes from E9.5-E17.5 embryos. $^{†}P < .01$ (unpaired t test, B) $*P < .05$ vs E9.5, $^{†}P < .05$ vs E10.5, (one-way ANOVA, Tukey's post hoc, D)
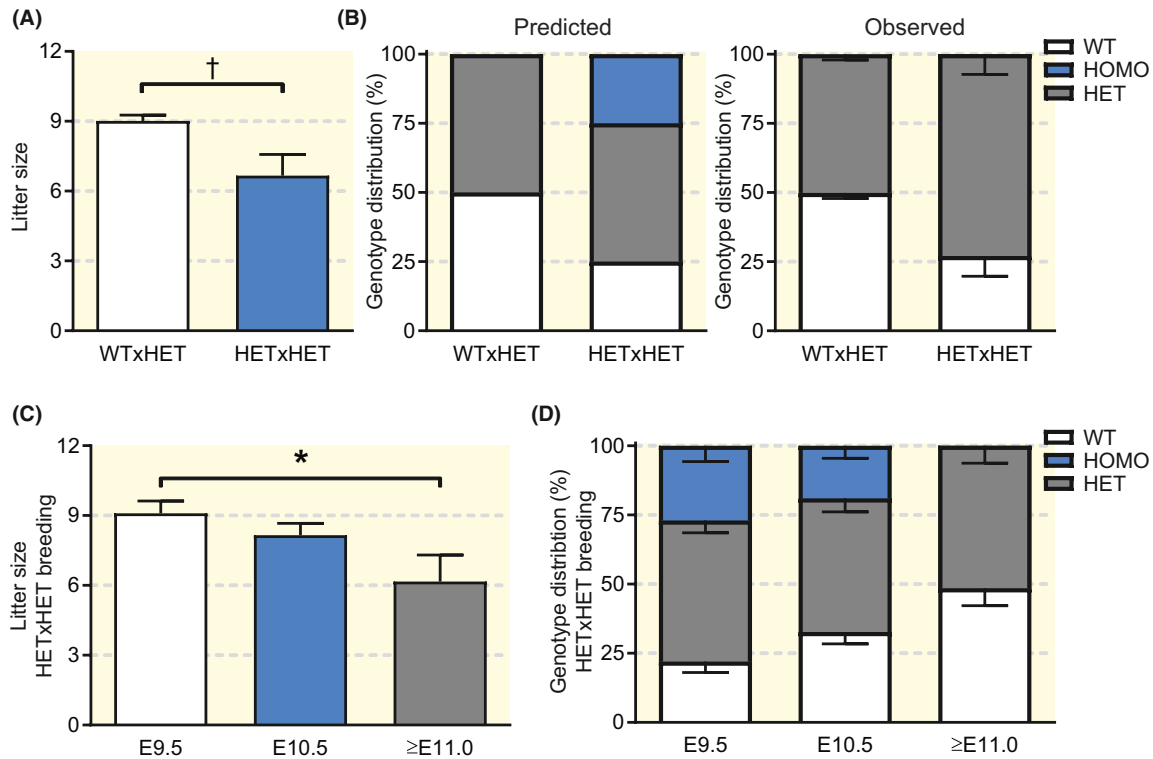
$Scn5a$-1798insD$^{-/-}$ (HOMO) embryos. A mean litter size of 9.0 ± 0.24 (n = 104 litters) was observed when crossing a heterozygous $Scn5a$-1798insD$^{+/-}$ (HET) male with a WT female (WTxHET breeding). In contrast, a significantly smaller mean litter size of 6.7 ± 0.91 (n = 12 litters; $P < .01$) was observed when crossing two HET animals (HETxHET breeding, Figure 3A). Moreover, while a Mendelian distribution of 25% WT, 50% HET and 25% HOMO animals would be expected in HETxHET breeding, a distribution of 28% WT, 72% HET and 0% HOMO animals was observed at birth (n = 9 litters, Figure 3B). This absence of HOMO pups and the shift in genotype ratio at birth indicate prenatal death of HOMO mice during development.

To investigate the exact time point of prenatal death, we assessed survival of HOMO mice (HETxHET breeding) during embryonic development at E9.5 (n = 11 litters), E10.5 (n = 19 litters) and E11.0 and older (n = 6 litters). While litter size was still the same as in WTxHET breeding at E9.5, litters from HETxHET breeding became significantly smaller throughout development (Figure 3C). Also, while HOMO embryos were still observed at a Mendelian rate at E9.5, no

live HOMO embryos were observed from E11.0 onwards (Figure 3D). At E10.5, some live, necrotic, and/or resorbed HOMO embryos were observed, indicating that HOMO embryos die around this stage of development. Embryonic death was never observed in HET or WT embryos. Overall, these findings indicate that homozygosity for the $Scn5a$-1798insD mutation results in embryonic lethality around 10.5.

2.3 | Homozygous $Scn5a$-1798insD embryos display slowed ventricular activation at E9.5 and E10.5

To investigate the potential mechanisms underlying embryonic lethality as a consequence of the mutation, we investigated WT and HOMO cardiac activity in more detail at E9.5 and E10.5. At E9.5, video recordings of intact embryos were performed. Ventricular beat duration was found to be significantly longer in HOMO as compared to WT hearts (WT: 710.9 ± 100.7 ms, n = 4 vs HOMO: 1168.0 ± 116.8 ms, n = 6; $P < .05$, Figure 4A), indicating that cardiac conduction in HOMO hearts is altered at E9.5.

FIGURE 3 Embryonic survival during developmental stages in $Scn5a$-1798insD$^{+/-}$ crossing. A, Average litter size at birth when crossing a heterozygous $Scn5a$-1798insD$^{+/-}$ (HET) male with a wild type (WT) female (WTxHET breeding; n = 104 liters) or two HET animals (HETxHET breeding; n = 12 litters). B, Predicted and observed genotype distribution of WT, HET and $Scn5a$-1798insD$^{-/-}$ (HOMO) animals at birth in HETxHET breeding (n = 9 litters). Prediction is according to Mendelian inheritance. C, Average litter size during early embryonic development in HETxHET breeding at E9.5 (n = 11 litters), E10.5 (n = 19 litters) and E11.0 and older (n = 6 litters). D, Distribution of embryo genotypes during early embryonic development. $^{†}P < .01$ (unpaired t test, A), $^{*}P < .05$ (one-way ANOVA, Tukey's post hoc, C)
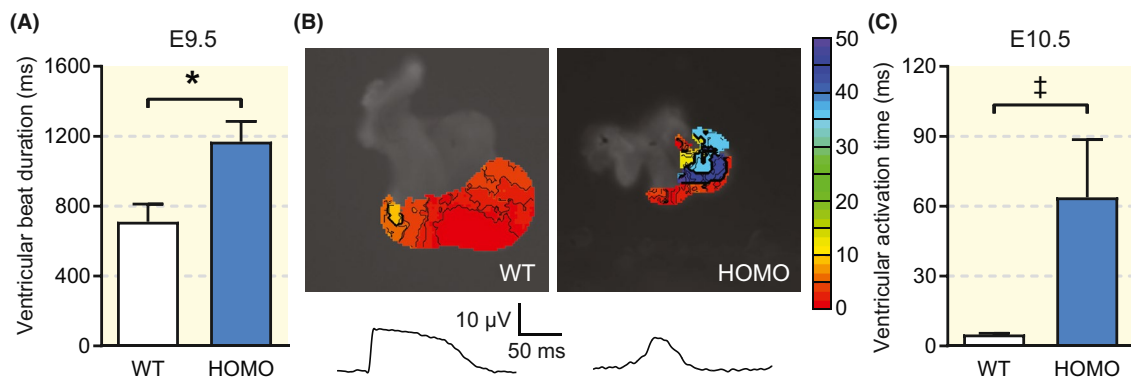
FIGURE 4 Effect of the homozygous $Scn5a$-1798insD mutation in hearts at E9.5 and E10.5. A, Ventricular beat duration in wild type (WT; n = 4) and $Scn5a$-1798insD$^{-/-}$ (HOMO; n = 6) embryonic hearts. B and C, Effect of the $Scn5a$-1798insD mutation in E10.5 hearts. Typical examples of optical maps and action potentials (B) and average activation time (C) of WT (n = 14) and HOMO (n = 3) hearts from embryos aged E10.5. $^{*}P < .05$, $^{‡}P < .0001$ (unpaired t test)

Optical mapping on WT and HOMO isolated hearts were performed at E10.5. In E10.5 WT hearts, organized ventricular activation patterns with fast ventricular activation times (4.9 ± 0.5 ms, n = 14) were observed. In contrast, HOMO ventricles at E10.5 activated extremely slow (mean activation time 63.8 ± 24.8 ms, n = 3; $P < .0001$) and in a chaotic manner (Figure 4B,C). Also, while action potentials in WT hearts displayed rapid upstrokes and long action potential duration at E10.5, action potentials in HOMO hearts had relatively slow upstrokes and typically a short action potential duration (Figure 4B). Of note, these overt electrical abnormalities in HOMO E10.5 hearts were accompanied by clear structural alterations and hearts were typically small in size and possibly necrotic (Figure 4B).

2.4 | Homozygous *Scn5a*-1798insD embryos display structural abnormalities at E9.5

In addition to electrical disturbances, we also investigated the impact of Na$_V$1.5 dysfunction on cardiac structural development. At E10.5, HOMO hearts were visibly smaller than WT hearts, and presence of pericardial oedema was observed in most HOMO embryos (Figure 5A), indicating poor cardiac function.[19] Moreover, most E10.5 hearts appeared to be

necrotic, while at E11.5 all embryos were clearly necrotic. At E9.5, HOMO hearts appeared to have a more tube-like morphology, suggesting delayed embryonic development. To investigate this in more detail, we identified cardiac tissue in sections from E9.5 embryos by immunostaining with an antibody against the cardiomyocyte-specific protein α-actinin, and quantified α-actinin-positive area as cardiac tissue volume (Figure 5B,C). This cardiac tissue volume analysis revealed that hearts of HOMO embryos were significantly
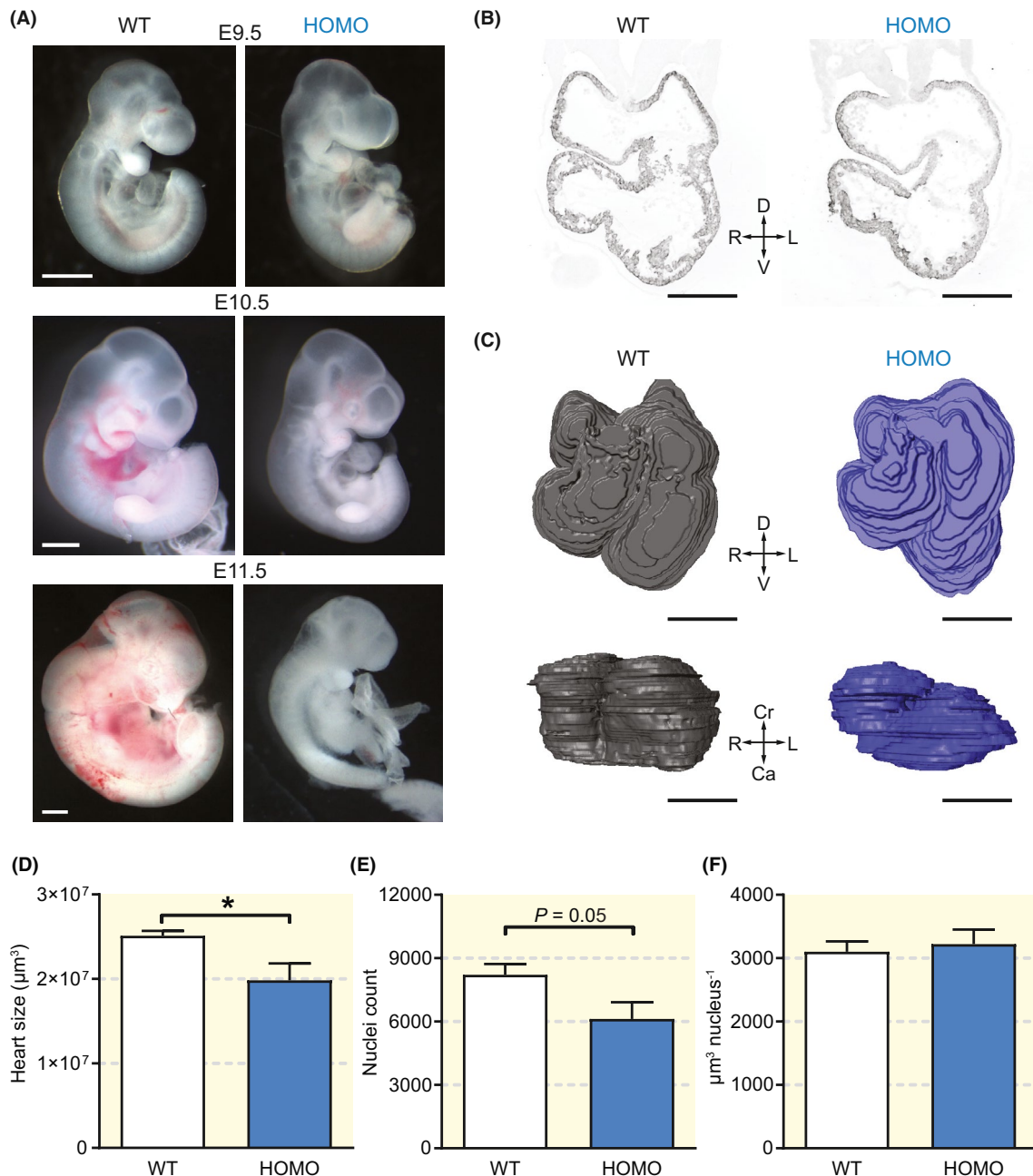
FIGURE 5 Structural effects of the *Scn5a*-1798insD mutation. A, Typical wild type (WT) and *Scn5a*-1798insD$^{-/-}$ (HOMO) embryos aged E9.5, E10.5 and E11.5 (scale bar: 500 μm). Cardiac abnormalities, pericardial oedema and necrosis can be observed in HOMO. B,C: Typical cardiac-specific α-actinin immunostaining in a WT and HOMO E9.5 embryo (B) and 3D reconstructions of cardiac tissue, based on α-actinin-positive area in immunostainings (C); scale bar: 200 μm. D-F, Analyses of cardiac structure in WT (n = 6) and HOMO (n = 6) hearts at E9.5. Average cardiac tissue volume (D), total cardiac nuclei count (E), and cardiac tissue volume per nucleus (F). *P < .05 (unpaired *t* test)

smaller than those of their WT littermates (WT: $25.1 \pm 0.7 \times 10^6$ μm^3, n = 6 vs HOMO: $19.8 \pm 2.0 \times 10^6$ μm^3, n = 6; $P < .05$, Figure 5D). In addition, a tendency to a reduction in total cardiomyocyte nuclei count was detected (WT: 8216 ± 511, n = 6 vs HOMO 6125 ± 793, n = 6; $P = .05$, Figure 5E), while no significant effect on cardiac volume per nucleus was observed (WT: 3102.0 ± 164.3 μm^3 nucleus^{-1}, n = 6 vs HOMO: 3222.0 ± 230.1 μm^3 nucleus^{-1}, n = 6; $P = $ NS, Figure 5F). Hence, the reduced cardiac volume in HOMO hearts appeared to be the result of a lower number of cardiomyocytes. Since these alterations in cardiac structure and development occurred at a developmental time point when I_{Na} is not yet functionally relevant (ie, at E9.5), this indicates the involvement of a non-electrogenic mechanism independent of I_{Na}.

3 | DISCUSSION

In this study, we demonstrate that in the embryonic murine heart, I_{Na} is functionally relevant for cardiac electrical activity at E10.5, but not at E9.5. Embryonic death of homozygous $Scn5a$-1798insD$^{-/-}$ (HOMO) mice occurred in utero around E10.5, and was preceded by impaired cardiac development and function at E9.5. Therefore, we here show that $Scn5a$/Na$_V$1.5 affects cardiac development before I_{Na} becomes functionally relevant for cardiac electrical activity, indicating a non-electrogenic role for Na$_V$1.5 in embryonic cardiac development.

3.1 | Functional relevance of Na$_V$1.5 for cardiac conduction during embryonic development

From E8.5 to E10.5 the embryonic murine heart develops from a primitive heart tube to a heart with four discernible chambers.[13] Physiological processes, such as cardiomyocyte contractility and intracardiac hemodynamics act as epigenetic factors mediating the development and morphogenesis of the embryonic heart.[20,21] Moreover, Radisic et al (2004) showed that electrical stimulation induces cardiomyocyte alignment and coupling in vitro and is therefore essential in ultrastructural organization.[22] The embryonic heart starts to contract around E8.5.[13,23] The electrophysiological mechanisms driving these first heart beats is disputed, with some studies pointing to intracellular calcium oscillations and the sodium-calcium exchanger (NCX) as the major drivers of cardiac activation,[16,24,25] while others demonstrated a crucial role for the L-type calcium current.[13,14] Na$_V$1.5 is present in the embryonic murine heart as early as E8.5-9.5.[12-14] However, it has been demonstrated in mice and other species that the cardiomyocyte membrane potential is relatively depolarised during these early stages[15,17,26]

because of the absence of several potassium currents.[17] As a consequence, sodium channels remain in a closed state and cardiac electrical function during early heart development does not depend on I_{Na}.[13,16,17,26] While in several studies presence of I_{Na} at later stages was described, measurements were pooled from embryos aged E10.5-E12.5 vs E16.5-E18.5,[27] and E11.0-E13.0 vs E17.0-E20.0.[17] Moreover, patch-clamp experiments in these studies were performed on embryonic cardiomyocytes which were cultured for 18-48 hours after isolation, which is known to affect I_{Na} characteristics in cardiomyocytes of other species.[28]

We here investigated the functional role of sodium channels by optical mapping, video recordings and patch-clamp measurements. These experiments were performed at specific embryonic developmental stages, directly after isolation of the embryo, thereby excluding variation because of pooling of various developmental stages and culturing of cardiomyocytes. Using the I_{Na} blocker TTX, we demonstrated that I_{Na} is irrelevant for cardiac electrical function at E9.5, but is functionally relevant from E10.5 onwards. Although at the concentration used (30 $\mu mol/L$), TTX is known to also inhibit neuronal sodium channels,[29] the latter are not available to activate at the depolarized resting membrane potential (~-40 mV) observed at E9.5,[30] and hence also not considered relevant at this early stage of development.

3.2 | Homozygous Na$_V$1.5 mutant mice generally die around E10.5

The $Scn5a$-1798insD$^{+/-}$ mouse model displays a mixed phenotype, comprising features of LQTS3, Brugada syndrome and cardiac conduction disease.[31,32] The $Scn5a$-1798insD mutation is located in an acid-rich C-terminal domain of Na$_V$1.5, and is surrounded by highly conserved residues.[33,34] In our study, $Scn5a$-1798insD$^{-/-}$ (HOMO) embryos were found to be present in a Mendelian distribution at E9.5, but absent or necrotic from E10.5 onwards. This time point of in utero death is in line with previous observations in other murine $Scn5a$ mutant models.[10,11] Embryonic death around E10.5 was observed in both a loss-of-function homozygous $Scn5a$ knockout mouse model,[10] and in mice carrying the gain-of-function ΔKPQ mutation.[11] Hence, $Scn5a$ mutations causing either gain-of-function or loss-of-function lead to embryonic death around the same developmental stage. The opposite effects of these mutations on the electrogenic function of sodium channels while embryonic death occurs at the same developmental age points to a non-electrogenic mechanism through which Na$_V$1.5 acts on embryonic development, independent of its electrical function.

Na$_V$1.5 forms a macromolecular complex with interacting proteins and these interactions modulate Na$_V$1.5 subcellular localization and function.[35,36] Similar to mutant

$Na_V1.5$ and deficiency, mutations in several $Na_V1.5$ interacting proteins result in embryonic death around the same developmental stage.[37-39] Strikingly, embryonic lethality was only observed in embryos with mutant $Na_V1.5$ interacting proteins, which are located at the intercalated discs of adult cardiomyocytes, including Coxsackievirus and adenovirus receptor and Plakophilin-2.[37-39] In contrast, mutant $Na_V1.5$ interacting proteins located at the lateral membranes of adult cardiomyocytes, such as dystrophin and syntrophin, do not show embryonic lethality.[40-42] Accordingly, the homozygous mutations $Scn5a$-D1275N and $Scn5a$-ΔSIV result in I_{Na} loss mainly at the lateral membrane and these mice are viable.[43,44] However, whole cell I_{Na} was moderately affected in these models, 77.2% and 49.2% respectively, which could also underlie the absence of embryonic lethality.[43,44]

In adult cardiomyocytes, $Na_V1.5$ forms a macromolecular complex with many intercalated disc-specific proteins, including the cytoskeletal adaptor protein Ankyrin-G.[45] Crucially, associations between $Na_V1.5$ and gap junctional Cx43,[45-47] desmosomal Plakophilin-2,[45,48] and adherens junctional Plakoglobin[47] have been described. Additionally, it has been found that $Na_V1.5$ dysfunction results in reduced levels of the cellular adhesion protein N-cadherin.[49] While embryonic cardiomyocytes lack distinct intercalated discs,[50] above observations show that $Na_V1.5$ interacts with proteins that are essential in the formation of intercalated disc structures. Also, since there is an overlap in localization of $Na_V1.5$ and other intercalated disc proteins, these proteins potentially co-traffic. Therefore, $Na_V1.5$ localization may play a central role in the formation of the intercalated disc region of cardiomyocytes and is thereby essential for correct cardiac development and embryonic survival. Moreover, cardiomyocyte elongation initiates during early embryonic development,[50] and it has been described that this elongation process is promoted by electrical activity.[22] While intercalated discs fully form at later stages, it is possible that $Na_V1.5$ dysfunction impairs the process of cardiomyocyte elongation and ultimately the formation of intercalated discs. Alternatively, a dose dependent effect could play a role, as it has been described that I_{Na} generated at the intercalated discs of adult cardiomyocytes is much larger than at the lateral membrane.[51] Therefore, loss of I_{Na} at the intercalated disc region likely results in a substantially bigger loss of total I_{Na}.

3.3 | Homozygous *Scn5a*-1798insD mice show electrical and morphological abnormalities before $Na_V1.5$ is functionally relevant

Embryonic mice homozygous for *Scn5a*-1798insD display delayed cardiac activation at E9.5. Our results here show that I_{Na} becomes functionally relevant at E10.5 and we therefore propose that delayed activation in the HOMO mice is because of structural abnormalities driven by non-electrogenic effects of $Na_V1.5$ on cardiac development. These effects of *Scn5a*/$Na_V1.5$ independent of I_{Na} have previously been described in zebra fish,[9] but were yet to be described in mammals. Indeed, cardiac tissue volume measurements on E9.5 embryos showed HOMO hearts were significantly smaller than those of WT littermates. We found a tendency to a reduction of nuclei count in cardiac tissue, while cardiac volume per nucleus was equal between WT and HOMO hearts, indicating that the reduction in cardiac volume in HOMO embryos is driven by a lower number of cardiomyocytes in the heart rather than a decreased cellular volume. A similar mechanism is described in zebra fish by Chopra and colleagues (2010),[9] where knockdown of the *Scn5a* homologs *scn5Laa* and/or *scn5Lab* led to decreased expression of the myocardial precursor genes *nkx2-5*, *gata4* and *hand2* in the anterior lateral mesoderm, resulting in impaired cardiac development and cardiomyocyte proliferation.[9] Surprisingly, these myocardial precursor genes were also reduced upon knockdown of *mog1*, a $Na_V1.5$ interacting protein and regulator of $Na_V1.5$ trafficking.[52] Therefore, it is possible that $Na_V1.5$/*Scn5a* dysfunction has similar effects on the expression of genes important in myocardial progenitors and consequently leads to impaired cardiac development. Other potential mechanisms explaining abnormal embryonic cardiac development in the setting in $Na_V1.5$ dysfunction include faulty trafficking of ion channels that form a trafficking complex with $Na_V1.5$, such as Kir2.1,[53] and/or altered localization of $Na_V1.5$ interacting proteins leading to impaired intercalated disc formation.

These non-canonical effects of $Na_V1.5$ on heart development shine a new light on how $Na_V1.5$ impacts on cardiac structure. Various structural abnormalities, such as dilated cardiomyopathy,[2-5] cardiac hypertrophy,[4,6] and cardiac fibrosis[4,7] have been observed in patients carrying heterozygous *SCN5A* mutations, potentially increasing the risk for cardiac arrhythmias and sudden cardiac death. These structural effects of $Na_V1.5$ dysfunction cannot be explained solely by the electrogenic alterations induced by these mutations, similar to our current observations in *Scn5a*-1798insD$^{-/-}$ embryos. Thus, non-electrogenic actions of $Na_V1.5$/*Scn5a* add to the complexity of cardiac sodium channel dysfunction, warranting further investigation of the underlying mechanisms.

In conclusion, we here provide evidence that $Na_V1.5$ affects cardiac development before I_{Na} is functionally relevant for cardiac electrical function, indicating that $Na_V1.5$ affects heart development in a non-electrogenic manner. The mechanisms underlying these non-electrogenic effects of $Na_V1.5$ remain to be investigated further and may be of particular relevance in understanding how $Na_V1.5$ dysfunction may lead to cardiac structural abnormalities.

4 | MATERIALS AND METHODS

4.1 | Generation and breeding of mice

Heterozygous $Scn5a$-1798insD$^{+/-}$ mice on a FVB/NRj background were used from our internal breeding programme. For details on generation of mice, see Remme et al (2006).[32] The mice had ad libitum access to Teklad 2916 chow (Envigo, Huntingdon, UK) and water. All experimental procedures were in accordance with governmental and institutional guidelines and approved upon by the local animal ethics committee (license number 103084-2). Heterozygous $Scn5a$-1798insD$^{+/-}$ mice aged 3-7 months were crossed to generate homozygous $Scn5a$-1798insD$^{-/-}$ embryos. Breeding couples were put together at the end of the afternoon and separated the next morning, after which the female was examined for the presence of a vaginal plug; if positive, this moment was considered as time point E0.5. An echo was performed 7 days later to confirm pregnancy. Patch clamp experiments were performed on cells of a $Tbx3^{Venus/+}$ mouse line on a FVB/NJ background.[18,54]

4.2 | Harvesting of embryos

Pregnant female mice were euthanized by CO_2 administration followed by cervical dislocation. Embryos were isolated and kept at 37°C in modified Tyrode's solution containing (in mmol/L): 140 NaCl, 5.4 KCl, 1 $MgCl_2$, 1.8 $CaCl_2$, 5.5 glucose, 5.0 HEPES at pH 7.4 (NaOH). Depending on the experiment either the whole embryo was used or the heart was isolated.

4.3 | Optical mapping

Embryonic hearts were isolated and stored in modified Tyrode's solution at 37°C. Prior to the measurements, the heart was placed for 5 minutes in incubation solution containing the voltage sensitive fluorescent dye Di-4-ANEPPS (15 μmol/L, AnaSpec, Fremont, CA, US) and the excitation-contraction uncoupler Blebbistatin (10 μmol/L, Tocris, Bristol, UK) to prevent movement artefacts. Subsequently, the heart was placed in a custom-made bath, which was perfused at 37°C with modified Tyrode's solution containing Blebbistatin. In order to obtain a measure of transmembrane potential, Di-4ANEPPS was excited by light provided by a 5 W LED (510 ± 20 nm) and the fluorescent emission light was recorded by a 100×100 pixel CMOS sensor (Brainvision, Tokyo, JP). 2048 millisecond-recordings of fluorescent emission light from the embryonic heart in sinus rhythm were obtained using MICAM Ultima software (version 0902, Brainvision, Tokyo, JP). Optical action potentials were calculated from the fluorescent emission light intensity and activation maps were generated using these optical action potentials in Matlab software (version 15.0, Mathworks, Naticks, MA, US) running the custom made Maplab extension (version 1.50.233, Medical Physics Department, Academic Medical Centre, Amsterdam, NL). Local time of activation was determined at the maximum dV dt^{-1} (V_{max}), that is, at the steepest point in the upstroke of the optical action potential. For activation time, the area of first depolarization in the ventricle was set as zero, and ventricular activation time was determined by measuring the time between the first and last depolarization in the ventricle.

To assess the electrogenic contribution of I_{Na} to cardiac activation, tetrodotoxin (TTX; Alomone, Jerusalem, IL) was used in a concentration of 30 μmol/L to block I_{Na}.[55] Recordings were performed at BL and 2 minutes after washing in TTX.

Embryos not used for optical mapping measurements were stored in 4% of paraformaldehyde for immunohistological investigation.

4.4 | Microscopy and video recording

Directly after isolation, whole embryos were placed in a 4-wells plate containing modified Tyrode's solution at 37°C. Thirty-second video recordings were made of both sides of the embryo to allow for heart rate and heart beat duration assessments. Recordings were made at BL and after 2 minutes incubation with the sodium channel blocker TTX (30 μmol/L) or the L-type calcium channel inhibitor nifedipine (5 μmol/L; Sigma-Aldrich, St. Louis, MO, US).

4.5 | Single cell electrophysiology

4.5.1 | Cell preparation

Embryonic hearts (E9.5-E17.5) were micro-dissected, cut into small pieces containing either AVC/ventricles or right atrium/SAN, and single cells were isolated by enzymatic dissociation as we described previously in detail.[18,54] Single cells were stored in a modified Kraft-Brühe solution (37°C) containing (in mmol/L): 85 KCl, 30 K_2HPO_4, 5.0 $MgSO_4$, 20 glucose, 5.0 pyruvic acid, 5.0 creatine, 30 taurine, 5.0 β-hydroxybutyric acid, 5.0 succinic acid, 1% of BSA, 2.0 Na2ATP at pH 6.9 (KOH) for at least 30 minutes at room temperature before they were put into a recording chamber on the stage of an inverted microscope, and superfused with modified Tyrode's solution (37°C). Cells were isolated from a $Tbx3^{Venus/+}$ mouse line on a FVB/NJ background[18,54] and only GFP-negative cells were measured, thereby selecting for atrial and ventricular cardiomyocytes.

4.5.2 | Data acquisition

Action potentials and net membrane currents were recorded using the amphotericin-perforated patch-clamp technique with an Axopatch 200B amplifier (Molecular Devices, Sunnyvale, CA, US). Data acquisition, voltage control and analysis were accomplished using custom software, and potentials were corrected for the estimated liquid junction potential.[56] Pipettes (resistance 2-3 MΩ) were pulled from borosilicate glass capillaries and were heat polished. Cell membrane capacitance (C_m) was estimated by dividing the time constant of the decay of the capacitive transient in response to 5 mV hyperpolarizing voltage clamp steps from −40 mV by the series resistance. Signals were low-pass-filtered with a cut off frequency of 5 kHz, and digitized at 5 Hz (currents and non-stimulated current clamp measurements), and 40 kHz (stimulated action potentials).

4.5.3 | Action potentials and membrane currents

Action potentials and membrane currents were measured in modified Tyrode's solution; patch pipettes were filled with solution containing (in mmol/L): 125 K-gluconate, 20 KCl, 5 NaCl, 0.22 amphotericin B, 10 HEPES at pH 7.2 (KOH). Action potentials were elicited at 2 Hz by 3 ms, ~1.2x threshold current pulses through the patch pipette. The action potential measurements were alternated by a general voltage clamp protocol to elucidate the ionic mechanism underlying the action potential. Since relatively few viable cells could be obtained after the isolation process, no specific channel blockers or modified solutions were used during the voltage clamp experiments in order to enhance cell survival and to ensure that remaining cardiomyocytes in the recording chamber stay undistorted for biophysical analysis. Membrane currents were measured in response of 500 ms depolarizing and hyperpolarizing voltage clamp steps from a holding potential of −40 mV at a cycle length of 2 seconds. Maximum diastolic potential (MDP) was measured from the average of 10 consecutive action potentials. I_{Na} was defined as inwards current activated upon depolarization to the holding potential of −40 mV.[18,54]

4.6 | Cardiac volume measurements

Embryos were fixed with 4% of paraformaldehyde overnight, dehydrated and embedded in paraffin, and cut at 8 μm slice thickness. One in four sections were used for immunohistochemistry to identify the myocardium by an overnight incubation at room temperature with mouse-α-actinin (Sigma-Aldrich A9357, St. Louis, MO, US, diluted 1:400), followed by a 2-hour incubation at room temperature with a goat-anti-mouse antibody conjugated with Alexa 488 (Thermo Fisher, Waltham, MA, US, diluted 1:250). DAPI was used for staining nuclei (Thermo Fisher, Waltham, MA, US, diluted 1:1000). Labelling α-actinin-positive cardiac tissue, calculating volume and generating 3D reconstructions were performed using Amira Software (version 5.3.3, Thermo Fisher Scientific, Waltham, MA, US) as described before.[18] Cardiac nuclei count was determined using previously described custom software.[57]

4.7 | Statistical analysis

Statistical analyses were performed with GraphPad Prism software (version 8, GraphPad, San Diego, CA, US). Data were tested for normality and appropriate statistical test were used. For analysis between two groups with normally distributed data a (paired) Student's *t* test was used, while for non-normally distributed data sets a Mann-Whitney test was used for unpaired measurements and a Wilcoxon test for paired measurements. For comparison of three or more normally distributed data sets a one-way ANOVA and Tukey's multiple comparisons post hoc analyses were performed, while a Friedman test and Dunn's multiple comparisons post hoc test was used for non-normally distributed data. Statistical significance for differences in current-voltage curves were determined by performing a two-way repeated measures ANOVA in SigmaStat software (Version 3.5, Systat Software Inc, San Jose, CA, US). For all tests, a *P* value lower than .05 was considered statistically significant. Mean data are presented ± Standard Error of Mean.

CONFLICT OF INTEREST

The authors declare no conflicts of interest.

DATA AVAILABILITY STATEMENT

The data that support the findings of this study are available from the corresponding author upon reasonable request.

ORCID

Gerard A. Marchal (iD) https://orcid.org/0000-0002-7353-0235
Carol Ann Remme (iD) https://orcid.org/0000-0003-0095-0084

REFERENCES

1. Remme CA, Wilde AAM, Bezzina CR. Cardiac sodium channel overlap syndromes: different faces of SCN5A mutations. *Trends Cardiovasc Med*. 2008;18(3):78-87.
2. Olson TM, Keating MT. Mapping a cardiomyopathy locus to chromosome 3p22-p25. *J Clin Invest*. 1996;97(2):528-532.
3. McNair WP, Ku L, Taylor MRG, et al. SCN5A mutation associated with dilated cardiomyopathy, conduction disorder, and arrhythmia. *Circulation*. 2004;110(15):2163-2167.
4. Bezzina CR, Rook MB, Groenewegen WA, et al. Compound heterozygosity for mutations (W156X and R225W) in SCN5A associated with severe cardiac conduction disturbances and degenerative changes in the conduction system. *Circ Res*. 2003;92(2):159-168.
5. Gosselin-Badaroudine P, Moreau A, Chahine M. Nav1.5 mutations linked to dilated cardiomyopathy phenotypes: Is the gating pore current the missing link? *Channels*. 2014;8(1):90-94.
6. van Hoorn F, Campian ME, Spijkerboer A, et al. SCN5A mutations in Brugada syndrome are associated with increased cardiac dimensions and reduced contractility. *PLoS ONE*. 2012;7(8):e4203 7-e42037.
7. Coronel R, Casini S, Koopmann TT, et al. Right ventricular fibrosis and conduction delay in a patient with clinical signs of Brugada syndrome: a combined electrophysiological, genetic, histopathologic, and computational study. *Circulation*. 2005;112(18):2769-2777.
8. Royer A, van Veen TAB, Le Bouter S, et al. Mouse model of SCN5A-linked hereditary Lenègre's disease: age-related conduction slowing and myocardial fibrosis. *Circulation*. 2005;111(14):1738-1746.
9. Chopra SS, Stroud DM, Watanabe H, et al. Voltage-gated sodium channels are required for heart development in zebrafish. *Circ Res*. 2010;106:1342-1350.
10. Papadatos GA, Wallerstein PMR, Head CEG, et al. Slowed conduction and ventricular tachycardia after targeted disruption of the cardiac sodium channel gene Scn5a. *Proc Natl Acad Sci USA*. 2002;99(9):6210-6215.
11. Nuyens D, Stengl M, Dugarmaa S, et al. Abrupt rate accelerations or premature beats cause life-threatening arrhythmias in mice with long-QT3 syndrome. *Nat Med*. 2001;7:1021-1027.
12. Domínguez JN, de la Rosa A, Navarro F, Franco D, Aránega AE. Tissue distribution and subcellular localization of the cardiac sodium channel during mouse heart development. *Cardiovasc Res*. 2008;78(1):45-52.
13. Chen F, De Diego C, Chang MG, et al. Atrioventricular conduction and arrhythmias at the initiation of beating in embryonic mouse hearts. *Dev Dyn*. 2010;239(7):1941-1949.
14. Liang H, Halbach M, Hannes T, et al. Electrophysiological Basis of the First Heart Beats. *Cell Physiol Biochem*. 2010;25(6):561-570.
15. Couch JR, West TC, Hoff HE. Development of the action potential of the prenatal rat heart. *Circ Res*. 1969;24(1):19-31.
16. Sasse P, Zhang J, Cleemann L, Morad M, Hescheler J, Fleischmann BK. Intracellular Ca^{2+} oscillations, a potential pacemaking mechanism in early embryonic heart cells. *J Gen Physiol*. 2007;130(2):133-144.
17. Davies MP, An RH, Doevendans P, Kubalak S, Chien KR, Kass RS. Developmental changes in ionic channel activity in the embryonic murine heart. *Circ Res*. 1996;78:15-25.
18. Mohan RA, Mommersteeg MTM, Domínguez JN, et al. Embryonic Tbx3^{+} cardiomyocytes form the mature cardiac conduction system by progressive fate restriction. *Development*. 2018;145(17):dev167361.
19. Savolainen SM, Foley JF, Elmore SA. Histology atlas of the developing mouse heart with emphasis on E11.5 to E18.5. *Toxicol Pathol*. 2009;37(4):395-414.
20. Hove JR, Köster RW, Forouhar AS, Acevedo-Bolton G, Fraser SE, Gharib M. Intracardiac fluid forces are an essential epigenetic factor for embryonic cardiogenesis. *Nature*. 2003;421(6919):172-177.
21. Chi NC, Bussen M, Brand-Arzamendi K, et al. Cardiac conduction is required to preserve cardiac chamber morphology. *Proc Natl Acad Sci USA*. 2010;107:14662-14667.
22. Radisic M, Park H, Shing H, et al. Functional assembly of engineered myocardium by electrical stimulation of cardiac myocytes cultured on scaffolds. *Proc Natl Acad Sci USA*. 2004;101:18129-18134.
23. Ji RP, Phoon CKL, Aristizábal O, McGrath KE, Palis J, Turnbull DH. Onset of cardiac function during early mouse embryogenesis coincides with entry of primitive erythroblasts into the embryo proper. *Circ Res*. 2003;92(2):133-135.
24. Viatchenko-Karpinski S, Fleischmann BK, Liu Q, et al. Intracellular Ca^{2+} oscillations drive spontaneous contractions in cardiomyocytes during early development. *Proc Natl Acad Sci USA*. 1999;96(14):8259-8264.
25. Reppel M, Sasse P, Malan D, et al. Functional expression of the Na^+/Ca^{2+} exchanger in the embryonic mouse heart. *J Mol Cell Cardiol*. 2007;42(1):121-132.
26. Kato Y, Masumiya H, Agata N, Tanaka H, Shigenobu K. Developmental changes in action potential and membrane currents in fetal, neonatal and adult guinea-pig ventricular myocytes. *J Mol Cell Cardiol*. 1996;28(7):1515-1522.
27. Yu L, Gao S, Nie L, et al. Molecular and functional changes in voltage-gated Na^+ channels in cardiomyocytes during mouse embryogenesis. *Circ J*. 2011;75(9):2071-2079.
28. Nurmi A, Vornanen M. Electrophysiological properties of rainbow trout cardiac myocytes in serum-free primary culture. *Am J Physiol Integr Comp Physiol*. 2002;282(4):R1200-R1209.
29. Tsukamoto T, Chiba Y, Wakamori M, et al. Differential binding of tetrodotoxin and its derivatives to voltage-sensitive sodium channel subtypes ($Na_v1.1$ to $Na_v1.7$). *Br J Pharmacol*. 2017;174(21):3881-3892.
30. Inserra MC, Israel MR, Caldwell A, et al. Multiple sodium channel isoforms mediate the pathological effects of Pacific ciguatoxin-1. *Sci Rep*. 2017;7(1):42810.
31. Postema PG, Van Den Berg MP, Van Tintelen JP, et al. Founder mutations in the Netherlands: SCN5a 1795insD, the first described arrhythmia overlap syndrome and one of the largest and best characterised families worldwide. *Netherlands Heart J*. 1795insD;17:422-428.
32. Remme CA, Verkerk AO, Nuyens D, et al. Overlap syndrome of cardiac sodium channel disease in mice carrying the equivalent mutation of human SCN5A-1795insD. *Circulation*. 2006;114(24):2584-2594.
33. Wei J, Wang DW, Alings M, et al. Congenital long-QT syndrome caused by a novel mutation in a conserved acidic domain of the cardiac Na^+ channel. *Circulation*. 1999;99(24):3165-3171.
34. Dolz-Gaitón P, Núñez M, Núñez L, et al. Functional characterization of a novel frameshift mutation in the C-terminus of the Nav1.5 channel underlying a Brugada syndrome with variable expression in a Spanish family. *PLoS ONE*. 2013;8(11):e81493-e81493.

35. Abriel H. Cardiac sodium channel Nav1.5 and interacting proteins: Physiology and pathophysiology. *J Mol Cell Cardiol*. 2010;48(1):2-11.

36. Shy D, Gillet L, Abriel H. Cardiac sodium channel NaV1.5 distribution in myocytes via interacting proteins: the multiple pool model. *Biochim Biophys Acta - Mol Cell Res*. 2013;1833(4):886-894.

37. Dorner AA. Coxsackievirus-adenovirus receptor (CAR) is essential for early embryonic cardiac development. *J Cell Sci*. 2005;118(15):3509-3521.

38. Marsman RFJ, Bezzina CR, Freiberg F, et al. Coxsackie and adenovirus receptor is a modifier of cardiac conduction and arrhythmia vulnerability in the setting of myocardial ischemia. *J Am Coll Cardiol*. 2014;63(6):549-559.

39. Grossmann KS, Grund C, Huelsken J, et al. Requirement of plakophilin 2 for heart morphogenesis and cardiac junction formation. *J Cell Biol*. 2004;167(1):149-160.

40. Albesa M, Ogrodnik J, Rougier J-SS, Abriel H. Regulation of the cardiac sodium channel Nav1.5 by utrophin in dystrophin-deficient mice. *Cardiovasc Res*. 2011;89(2):320-328.

41. Gavillet B, Rougier J-S, Domenighetti AA, et al. Cardiac sodium channel Nav1.5 is regulated by a multiprotein complex composed of syntrophins and dystrophin. *Circ Res*. 2006;99(4):407-414.

42. Stevenson SA, Cullen MJ, Rothery S, Coppen SR, Severs NJ. High-resolution en-face visualization of the cardiomyocyte plasma membrane reveals distinctive distributions of spectrin and dystrophin. *Eur J Cell Biol*. 2005;84(12):961-971.

43. Watanabe H, Yang T, Stroud DM, et al. Striking in vivo phenotype of a disease-associated human scn5a mutation producing minimal changes in vitro. *Circulation*. 2011;124(9):1001-1011.

44. Shy D, Gillet L, Ogrodnik J, et al. PDZ domain-binding motif regulates cardiomyocyte compartment-specific Nav1.5 channel expression and function. *Circulation*. 2014;130(2):147-160.

45. Sato PY, Coombs W, Lin X, et al. Interactions between ankyrin-G, Plakophilin-2, and Connexin43 at the cardiac intercalated disc. *Circ Res*. 2011;109(2):193-201.

46. Jansen JA, Noorman M, Musa H, et al. Reduced heterogeneous expression of Cx43 results in decreased Nav1.5 expression and reduced sodium current that accounts for arrhythmia vulnerability in conditional Cx43 knockout mice. *Hear Rhythm*. 2012;9(4):600-607.

47. Noorman M, Hakim S, Kessler E, et al. Remodeling of the cardiac sodium channel, connexin43, and plakoglobin at the intercalated disk in patients with arrhythmogenic cardiomyopathy. *Heart Rhythm*. 2013;10(3):412-419.

48. Cerrone M, Lin X, Zhang M, et al. Missense mutations in plakophilin-2 cause sodium current deficit and associate with a Brugada syndrome phenotype. *Circulation*. 2014;129(10):1092-1103.

49. Te Riele ASJM, Agullo-Pascual E, James CA, et al. Multilevel analyses of SCN5A mutations in arrhythmogenic right ventricular dysplasia/cardiomyopathy suggest non-canonical mechanisms for disease pathogenesis. *Cardiovasc Res*. 2017;113(1):102-111.

50. Hirschy A, Schatzmann F, Ehler E, Perriard J-C. Establishment of cardiac cytoarchitecture in the developing mouse heart. *Dev Biol*. 2006;289(2):430-441.

51. Lin X, Liu N, Lu J, et al. Subcellular heterogeneity of sodium current properties in adult cardiac ventricular myocytes. *Hear Rhythm*. 2011;8(12):1923-1930.

52. Zhou J, Wang L, Zuo M, et al. Cardiac sodium channel regulator MOG1 regulates cardiac morphogenesis and rhythm. *Sci Rep*. 2016;6:21538.

53. Ponce-Balbuena D, Guerrero-Serna G, Valdivia CR, et al. Cardiac Kir2.1 and Na$_V$1.5 channels traffic together to the sarcolemma to control excitability. *Circ Res*. 2018;122(11):1501-1516.

54. van Eif V, Stefanovic S, van Duijvenboden K, et al. Transcriptome analysis of mouse and human sinoatrial node cells reveals a conserved genetic program. *Development*. 2019;146(8):dev173161.

55. Gellens ME, George AL, Chen LQ, et al. Primary structure and functional expression of the human cardiac tetrodotoxin-insensitive voltage-dependent sodium channel. *Proc Natl Acad Sci USA*. 1992;89(2):554-558.

56. Barry PH, Lynch JW. Liquid junction potentials and small cell effects in patch-clamp analysis. *J Membr Biol*. 1991;121:101-117.

57. de Boer BA, van den Berg G, Soufan AT, et al. Measurement and 3D-visualization of cell-cycle length using double labelling with two thymidine analogues applied in early heart development. *PLoS ONE*. 2012;7(10):e47719.